# ORIGINAL RESEARCH ARTICLE

# Drug-Drug Interaction Pattern Recognition

*John Z. Duan*

Office of New Drug Quality Assessment, Office of Pharmaceutical Science, Center for Drug Evaluation and
Research, Food and Drug Administration, Silver Spring, Maryland, USA

## Abstract

**Background and Objective:** Drug-drug interaction (DDI) is an important
aspect of drug development, especially for safety. When a drug is used
concomitantly with other drug(s), one of the major concerns is the change of
exposures, including the rate and extent of drug absorption, distribution,
metabolism and elimination. To address the concerns, a common practice is
to measure and report the differences between the exposure in the presence
and in the absence of concomitant medication (COMED). The area under
the plasma concentration versus time curve (AUC), maximum plasma con-
centration ($C_{max}$) and time to reach the $C_{max}$ ($t_{max}$) changes are usually
measured in DDI studies. A usual observation is the different extents of
changes among AUC, $C_{max}$ and $t_{max}$, which may raise concerns in certain
therapeutic areas or some special agents. The objective of this study was to
investigate the variation among changes of AUC, $C_{max}$ and $t_{max}$ in DDI
studies, and its pharmacokinetic manifestation.

**Data Sources:** Based on a list of DDI results from the literature, with the
assumptions that the primary parameters of a drug of interest were altered
during a DDI, two sets of simulated data were generated according to a single
oral dose, one-compartment model. The first set including 24 cases with dif-
ferent half-lives and absorption constants ($k_a$) considered the exposure
changes upon independent variation of bioavailability (F), clearance (CL),
volume of distribution ($V_d$) and $k_a$ up to 50-fold increases or decreases. The
second set considered the exposure changes with simultaneous variation of F,
CL, $V_d$, and $k_a$ within 5-fold range (increase or decrease) for a case selected
from the first set.

**Study Selection, Data Extraction and Synthesis:** Parameter fold changes
(defined in a fashion showing fold increase or fold decreases, including CL
fold change, F fold change, $V_d$ fold change and $k_a$ fold change) and exposure
changes (AUC fold change, $C_{max}$ fold change, $t_{max}$ fold change and fold
change difference [AUC fold change – $C_{max}$ fold change]) were used to gen-
erate plots demonstrating various relationships between parameter fold
changes and exposure changes. Based on the observations that AUC was
influenced by CL and F, $C_{max}$ was affected by all four parameters, $t_{max}$ was
mainly determined by CL and $k_a$, F did little for $t_{max}$ and $k_a$ was unrelated to
AUC, a chart was created for DDI pattern recognition.

**Conclusion:** An approach, named DDI pattern recognition, is proposed for didactical purposes. It provides a quick initial estimate for interpreting the DDI results based on the exposure changes. This approach entails the following stages: (i) performing a drug interaction study; (ii) calculating the exposure changes in the presence of COMED compared to those in the absence of COMED, and the fold change difference; (iii) selecting the parameter fold changes that may play important roles in a specific DDI, by estimating their possible ranges; and (iv) interpreting the DDI by integrating all the information available, such as the possible mechanism involved. A quicker and better understanding about the processes, which dominate a DDI, has been achieved using this approach by focusing on integration of all information available and mechanistic interpretation.

## Introduction

Drug-drug interaction (DDI) is an important aspect of drug development. When a drug is used concomitantly with other drug(s), one of the major concerns is the change of exposures, including the rate and extent of drug absorption, distribution, metabolism and elimination. To address these concerns, a common practice is to measure the exposure and report its increases (or decreases) when the drug is used in the presence of concomitant medication (COMED) compared to that when it is used alone.

*In vivo* DDI studies are generally designed in a crossover fashion to compare the exposures of the drug of interest with and without COMED. Most often, the differences of the exposures are based on the following three measures: (i) area under the plasma concentration versus time curve (AUC), a measure of the total exposure; (ii) maximum plasma concentration ($C_{max}$), a measure of the extent of the exposure; and (iii) time to the $C_{max}$ ($t_{max}$), a measure of the rate of the exposure.

These exposure measures are usually obtained by non-compartmental analysis,[1] which is simple and accurate. $C_{max}$ and $t_{max}$ are directly observed from the plasma concentration versus time curve. As long as the sampling times are appropriately selected, these two values can be adequately captured. If the sampling times are long enough, AUC is estimated from zero to the last measured timepoint (e.g. 24 hours after dosing) using the linear trapezoidal rule or elated methods,[1] such as log trapezoidal method. Usually, it is extrapolated from the last measured timepoint to infinity by incorporating the elimination rate constant, which describes the rate of drug removal from the body.[1]

When comparing the exposures between the presence and absence of COMED, a usual observation is the inconsistent changes between AUC and $C_{max}$ in a specific DDI study. For example, cases observed in the literature are presented in table I.

As seen, not only the exposure folds vary, but the relative folds between AUC and $C_{max}$ for the same interaction differ as well. Roughly, the relative fold changes between AUC and $C_{max}$ can be classified into three categories. In the first category, AUC and $C_{max}$ have similar fold changes during DDI.[2,3] The second category includes the cases in which AUC has larger fold changes compared to $C_{max}$.[4-8] In cases of the third category, $C_{max}$ has larger fold changes compared with AUC.[9-18]

It is interesting to note that rosuvastatin in three different studies with three different concomitant medications (gemfibrozil,[6] lopinavir/ritonavir[7] and ciclosporin,[8] respectively) showed similar pattern with $C_{max}$ having higher fold changes compared to AUC fold changes, although the absolute fold changes were different (2.21, 4.7 and 10.6 for $C_{max}$, respectively). On the

**Table I.** Exposure changes due to drug-drug interactions reported in the literature

| Drug of interest[a] | COMED | AUC fold[b] | $C_{max}$ fold[b] | $t_{max}$ change (h) | Reference |
|---|---|---|---|---|---|
| Erlotinib | Ketoconazole | 2 | 2 | −1.4 | 2 |
| Selegiline | Oral contraceptives | 10–20 | 10–20 | −0.25 | 3 |
| Paclitaxel | OC144-093 (ONT-093) | 1.5 | 2 | NR | 4 |
| Simvastatin | Imatinib | 2 | 3.5 | NR | 5 |
| Rosuvastatin | Gemfibrozil | 1.88 | 2.21 | −1 | 6 |
| Rosuvastatin | Lopinavir/ritonavir | 2.1 | 4.7 | −1.2 | 7 |
| Rosuvastatin | Ciclosporin | 7.1 | 10.6 | −1 | 8 |
| Everolimus | Ciclosporin[c] | 1.74 | 1.06 | 0.5 | 9 |
| Everolimus | Ciclosporin[d] | 2.68 | 1.82 | 0 | 9 |
| Paroxetine | Terbinafine | 2.5 | 1.9 | NR | 10 |
| Desipramine | Terbinafine | 5 | 2 | NR | 11 |
| Duloxetine | Fluvoxamine | 6 | 2.5 | NR | 12 |
| Levacetylmethadol | Ketoconazole | 5.29 | 3.22 | −0.09 | 13 |
| Atomoxetine | Paroxetine or fluoxetine | 6–8 | 3–4 | NR | 14 |
| Repaglinide | Gemfibrozil | 7.0 | 2.0 | NR | 15 |
| Sirolimus | Posaconazole | 8.9 | 6.7 | 1 | 16 |
| Saquinavir | Ritonavir | 128.9 | 32.5 | 0.8 | 17 |
| Salmeterol | Ketoconazole | 16 | 1.4 | NR | 18 |

a   This is the drug that is studied to determine if its exposure is changed by the presence of another drug, which is termed COMED.

b   AUC fold and $C_{max}$ fold are the ratios between the exposure in the presence of COMED and that in the absence of COMED. AUC fold = AUC (with COMED)/AUC (without COMED); $C_{max}$ fold = $C_{max}$ (with COMED)/$C_{max}$ (without COMED).

c   Sandimmune® formulation: a gelatin capsule filled with a corn oil suspension.

d   Neoral® formulation: a gelatin capsule filled with a microemulsion preconcentrate.

**AUC** = area under the plasma concentration vs time curve; **$C_{max}$** = maximum plasma concentration; **COMED** = concomitant medication; **NR** = not reported; **$t_{max}$** = time to $C_{max}$.

other hand, gemfibrozil as a COMED in another study[15] caused AUC and $C_{max}$ fold changes of repaglinide following another pattern: AUC was much higher than $C_{max}$ (7 vs 2). The difference was even larger in a study where salmeterol had 16-fold AUC in the presence of ketoconazole, whereas the $C_{max}$ fold change was only 1.4.[18] Also note that $t_{max}$ change was positive (increase) in some situations and negative (decrease) in others.

In some cases, AUC and $C_{max}$ changes could be in the opposite directions. For example, full dose of amprenavir and nelfinavir resulted in decrease in amprenavir $C_{max}$ by 14%, but increase in AUC by 46%.[19] In another report, 14 healthy volunteers (7 male, 7 female) received single oral 0.5 mg doses of the anticholinergic agent scopolamine in a randomized crossover fashion with either 250 mL of water or fresh-squeezed, single-strength grapefruit juice. In the presence of grapefruit juice, scopolamine $C_{max}$ was decreased 11%, while AUC was increased 35%, and time to peak level ($t_{max}$) was extended from 23.5 minutes to 59.5 minutes (153% increase)[20] compared with water.

This difference of fold changes between AUC and $C_{max}$ could be of concern. For certain drug effects, the $C_{max}$ is an important consideration while under other circumstances, AUC is important. If a clinical outcome is most closely related to drug concentration (e.g. tachycardia with sympathomimetics), the exposure measure, $C_{max}$, may be the most important to consider. Conversely, if the clinical outcome is related more to extent of exposure, AUC would be preferred[21] in the context that a long, low concentration exposure may be as important as shorter but higher concentration.

If we have a better understanding of this phenomenon, it will be greatly helpful to clinical interpretation of the observed DDI. Furthermore, if we can predict the relative change of AUC, $C_{max}$ and $t_{max}$ based on the information available, it will be more valuable. This study intends to make such an attempt for didactical purposes. By assuming that the DDI was a result of changes of primary parameters of the drug of interest, the relative changes of AUC, $C_{max}$ and $t_{max}$ were investigated by various simulations.

## Methods

The important steps of this study included: setting up the model and specifications; implementation of the model by simulations; and data analyses and result interpretations.

### The Assumptions

This study made the following assumptions.
1. DDI was considered as pharmacokinetic interaction and no pharmacodynamic interaction was involved.
2. DDI resulted in changes of one or more of the primary pharmacokinetic parameters of the drug of interest, such as absorption constant ($k_a$), bioavailability (F), volume of distribution ($V_d$) and clearance (CL), which, in turn, altered the secondary parameters, such as AUC, $C_{max}$ and $t_{max}$. Based on this assumption, COMED was not specified in all the simulations performed regarding its dosage amount, dosing time, dosing frequency and dose titration scheme. However, the changes of the primary parameters of the drug of interest were considered to be the reflections of the combinations of all these factors.
3. The pharmacokinetics were assumed to follow a single dose, one-compartment model with first-order absorption and first-order elimination for oral administration route.

### Pharmacokinetic Model

A pharmacokinetic model loosely based on midazolam *in vivo* characteristics was selected. The model was described by the formula in

equation (1):

$$C = \frac{F \bullet Dose \bullet k_a}{V_d(k_a - CL/V_d)} \bullet (e^{-CL/V_d \bullet t} - e^{-k_a \bullet t})$$

(Eq. 1)

where C is the plasma drug concentration at t, the time elapsed after the dosage administration of the amount (Dose).

This model and associated parameters were for the drug of interest only. For COMED, no specific model and parameters were needed according to assumption (2). The CL, F, $V_d$, and $k_a$ of the drug of interest would be changed to reflect the effects of COMED (see Simulations and Glossary sections).

### Simulations

The model parameters of CL and $V_d$ were selected from a collection of drugs with different half-lives.[22] As shown in figure 1, drugs with
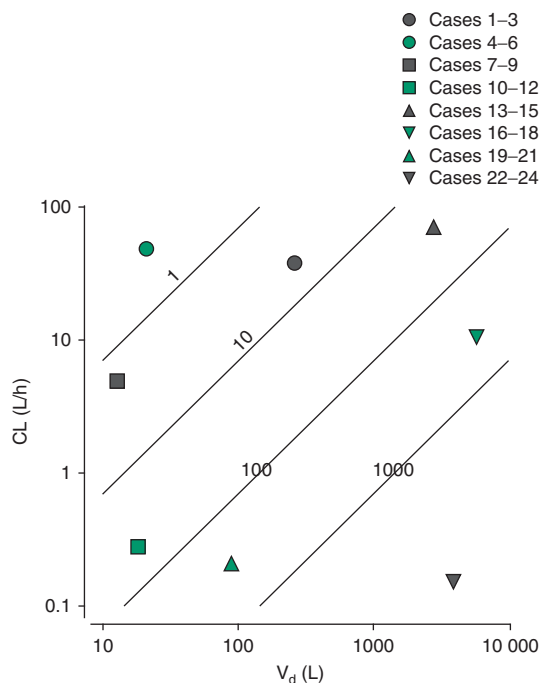


**Fig. 1.** The selection of parameters of clearance (CL) and volume of distribution ($V_d$). CL (y-axis) and $V_d$ (x-axis) vary widely. The diagonal lines show the combinations of CL and $V_d$ with the same half-lives (in hours, labeled near the lines). The selected combinations of parameters are represented by different symbols.

**Table II.** Model parameters cases

| Case # | F | $k_a$ (h$^{-1}$) | CL (L/h) | $V_d$ (L) | Half-life (h) |
|---|---|---|---|---|---|
| 1 | 0.2 | 0.2 | 38 | 260 | 4.74 |
| 2 | 0.2 | 1 | 38 | 260 | 4.74 |
| 3 | 0.2 | 5 | 38 | 260 | 4.74 |
| 4 | 0.2 | 0.2 | 48 | 20.8 | 0.30 |
| 5 | 0.2 | 1 | 48 | 20.8 | 0.30 |
| 6 | 0.2 | 5 | 48 | 20.8 | 0.30 |
| 7 | 0.2 | 0.2 | 4.88 | 12.8 | 1.82 |
| 8 | 0.2 | 1 | 4.88 | 12.8 | 1.82 |
| 9 | 0.2 | 5 | 4.88 | 12.8 | 1.82 |
| 10 | 0.2 | 0.2 | 0.28 | 18 | 44.55 |
| 11 | 0.2 | 1 | 0.28 | 18 | 44.55 |
| 12 | 0.2 | 5 | 0.28 | 18 | 44.55 |
| 13 | 0.2 | 0.2 | 68 | 2800 | 28.54 |
| 14 | 0.2 | 1 | 68 | 2800 | 28.54 |
| 15 | 0.2 | 5 | 68 | 2800 | 28.54 |
| 16 | 0.2 | 0.2 | 11 | 5800 | 365.40 |
| 17 | 0.2 | 1 | 11 | 5800 | 365.40 |
| 18 | 0.2 | 5 | 11 | 5800 | 365.40 |
| 19 | 0.2 | 0.2 | 0.2 | 88 | 304.92 |
| 20 | 0.2 | 1 | 0.2 | 88 | 304.92 |
| 21 | 0.2 | 5 | 0.2 | 88 | 304.92 |
| 22 | 0.2 | 0.2 | 0.158 | 3880 | 17 018 |
| 23 | 0.2 | 1 | 0.158 | 3880 | 17 018 |
| 24 | 0.2 | 5 | 0.158 | 3880 | 17 018 |

**CL** = clearance; **F** = bioavailability; **$k_a$** = absorption rate constant; **$V_d$** = volume of distribution.

various combination values of CL and $V_d$ were located in several half-life zones.[22] One or two combinations (in case of two, one with higher CL and another with lower CL with similar half-lives) of CL and $V_d$ values were selected from each zone.

For each combination of CL and $V_d$, there were three levels of $k_a$ values (0.2, 1 and 5 h$^{-1}$, respectively). F value was chosen as 0.2. There were a total of 24 cases as summarized in table II.

For each case, the model parameters and the simulation specifications varied as shown in table III for Case 2 as an example. Other cases used the same values except the second column ('Value'). The 'Value' column was referred to the parameter values when the drug of interest was administered alone. When this drug was administered with COMED, these parameters would change. The possible values after change

are listed in the third column ('Values with COMED'). Twenty-five simulations were conducted for each of the four parameters (CL, F, $k_a$ and $V_d$) in each of the 24 cases. Therefore, there were a total of 2400 simulations conducted.

The time values were selected from the interval between 0 to 580 hours for the first 15 cases. The rest of the cases used much longer intervals (58 000 hours for Cases 16–21 and 580 000 hours for the last three cases). These intervals were chosen with a consideration that most of the simulated profiles would be captured in order to get a relatively accurate AUC calculation by using trapezoidal method (zero to last timepoint). To get a smooth curve and relatively more accurate AUC, the interval between two adjacent timepoints was chosen to be 0.1 hours.

Simulations were conducted for each of the values of CL, F, $V_d$ and $k_a$ using R program (version 2.8, R project group). For every scenario, concentration-time profile was generated and the $C_{max}$, $t_{max}$ and AUC were calculated.

R packages including 'base', 'stats', 'graphics' and 'lattice' were used for AUC, $C_{max}$ and $t_{max}$ calculations, and for plotting the data. Several functions were defined, such as AUC to last timepoint ($AUC_t$) and AUC to infinity ($AUC_\infty$) according to the trapezoid rule as shown in equations (2) and (3).

$$AUC_t = \int_0^t C \bullet dt \approx \Delta t \bullet (C_{t0}/2 + C_{t1}$$
$$+ C_{t2} + \cdots + C_t/2) \quad \text{(Eq. 2)}$$

$$AUC_\infty = \frac{C_t}{(CL/V_d)} + AUC_t \quad \text{(Eq. 3)}$$

where $C_{t0}$, $C_{t1}$, …, $C_t$ refer to the concentrations at initial timepoint (0), timepoint 1 and so on, until timepoint t.

$C_{max}$ and $t_{max}$ were identified by R using max() function. The values of AUC, $C_{max}$ and $t_{max}$ were calculated for each scenario.

To investigate the situation where different parameters changed simultaneously, another set of simulations was conducted for Case 2, in which every combination of the four parameter fold changes were simulated as shown in table IV. In

**Table III.** Simulation model parameters

| Parameter | Value | Values with COMED | Justification |
|---|---|---|---|
| Dose (mg) | 5 | 5 | One of the midazolam clinical doses |
| $k_a$ (1/h) | 1 | 0.02, 1/n11,…, 1/n1, 1, n1×1,…, n11×1, 50[a] | Low (1/50) to high (50×) around 1 |
| F | 0.2 | 0.04, 0.2/n11,…, 0.2/n1, 0.2, n1×0.2,…, n11×0.2, 1.0[b] | Low (1/5) to high (5×) around 0.2 |
| CL (L/h) | 38 | 0.76, 38/n11,…, 38/n1, 38, n1×38,…, n11×38, 1900[a] | Low (1/50) to high (50×) around 38 |
| $V_d$ (L) | 260 | 0.11, 260/n11,…, 260/n1, 260, n1×260,…, n11×260, 13 000[a] | Low (1/50) to high (50×) around 260 |

a  n1, n2, ..., n10, n11 represent 11 numbers from 1 to 50, evenly spaced between subsequent numbers. Therefore, there are a series of 25 numbers centered at the defaults shown in the 'Value' column. On the right side, there are 12 numbers greater than the defaults (the 'Value'), which are n1×Value, n2×Value, …, n10×Value, n11×Value, and 50×Value. On the left side, there are another 12 numbers, which are fractions of the Value: Value/50, Value/n11, Value/n10, …, Value/n2, and Value/n1.

b  n1, n2, ..., n10, n11 have the similar meaning as in footnote a except that they represent 11 numbers from 1 to 5 considering the bioavailability limit (0 to 1).

**CL** = clearance; **COMED** = concomitant medication; **F** = bioavailability; **$k_a$** = absorption rate constant; **$V_d$** = volume of distribution.

table IV, each parameter had five levels and there were 625 ($5^4$) possible combinations. Similar to the first set, simulations were conducted using the R program. For every scenario, the concentration-time profile was generated, and the $C_{max}$, $t_{max}$ and AUC were calculated.

### Glossary

To facilitate the discussion, it would be beneficial to define certain terms used in this study.

**Standard Parameters**. The standard setting for the simulation, the scenario where no COMED was used and the parameters of the drug of interest were not changed. For example of Case 2, the standard setting was given in the second column of table III: CL = 38 h/L, F = 0.2, $k_a$ = 1 $h^{-1}$ and $V_d$ = 260 L. The standard parameters for other cases can be found in table II.

**Parameter Fold Changes**. The ratios of the parameters in a specific simulation scenario to those of the standard setting when the parameters were not less than the standard parameters. Otherwise (i.e. the parameters in simulation were less than the standard parameters), they were referred to the negative ratios of the standard parameters to the parameters used in a simulation scenario. For example, the CL fold change was defined as the ratios of the CL used for a specific simulation to the standard CL (e.g. 38 L/h for Case 2) when CL was not less than the standard. If CL is less than the standard, the CL fold change was defined as the negative ratio

of the standard CL (38 L/h for Case 2) to the CL used in the simulation ($CL_{sim}$) as shown in equation (4).

$$\text{When } CL_{sim} \geq 38,$$
$$\text{CL fold change} = CL_{sim}/38$$
$$\text{When } CL_{sim} < 38,$$
$$\text{CL fold change} = -38/CL_{sim}$$
$$\text{(Eq. 4)}$$

where $CL_{sim}$ was the value of CL in a specific simulation scenario.

Similarly, F fold change was defined as shown in equation (5).

$$\text{When } F_{sim} \geq 0.2,$$
$$\text{Ffold change} = F_{sim}/0.2$$
$$\text{When } F_{sim} < 0.2,$$
$$\text{Ffold change} = -0.2/F_{sim}$$
$$\text{(Eq. 5)}$$

where $F_{sim}$ was the value of F in a specific simulation scenario.

$V_d$ fold change was defined as shown in equation (6).

$$\text{When } V_{d,sim} \geq 260,$$
$$V_d \text{ fold change} = V_{d,sim}/260$$
$$\text{When } V_{d,sim} < 260,$$
$$V_d \text{ fold change} = -260/V_{d,sim}$$
$$\text{(Eq. 6)}$$

where $V_{d,sim}$ was the value of $V_d$ in a specific simulation scenario.

$k_a$ fold change was defined as shown in equation (7).

When $k_{a,sim} \geq 1$,

$$k_a \text{ fold change} = k_{a,sim}/1$$

When $k_{a,sim} < 1$,

$$k_a \text{ fold change} = -1/k_{a,sim}$$

(Eq. 7)

where $k_{a,sim}$ was the value of $k_a$ in a specific simulation scenario.

Note that the standard parameters for Case 2 (CL = 38 L/h, F = 0.2, $k_a$ = 1 h$^{-1}$ and $V_d$ = 260 L) were used for illustration purpose. A set of specific standard parameters (see table II) were used in each specific case.

In this study, F fold changes were set at −5…,1, …, 5. The other parameter fold changes (CL fold change, $V_d$ fold change and $k_a$ fold change) were set to −50, …, 1, …, and 50, for the first set of simulations (see table III) and −5, −2, 1, 2, 5 for the second set of simulations (see table IV).

**Standard Exposures**. The exposures resulted from the standard parameters (defined above), including standard $AUC_\infty$ ($AUC_{\infty,std}$), standard $C_{max}$ ($C_{max,std}$) and standard $t_{max}$ ($t_{max,std}$).

**Exposure Changes**. The ratios of the exposures resulted from a simulated scenario to the standard exposures (defined above). The AUC fold change and $C_{max}$ fold change were defined in a fashion similar to parameter fold changes as shown in equations (8) and (9).

When $AUC_{\infty,sim} \geq AUC_{\infty,std}$,

$$AUC \text{ fold change} = AUC_{\infty,sim}/AUC_{\infty,std}$$

When $AUC_{\infty,sim} < AUC_{\infty,std}$,

$$AUC \text{ fold change} = -AUC_{\infty,std}/AUC_{\infty,sim}$$

(Eq. 8)

where $AUC_{\infty,sim}$ was the value of $AUC_\infty$ in a specific simulation scenario.

When $C_{max,sim} \geq C_{max,std}$,

$$C_{max} \text{ fold change} = C_{max,sim}/C_{max,std}$$

When $C_{max,sim} < C_{max,std}$,

$$C_{max} \text{ fold change} = -C_{max,std}/C_{max,sim}$$

(Eq. 9)

where $C_{max,sim}$ was the value of $C_{max}$ in a specific simulation scenario.

Please note that by using fold changes, the increases were represented by the number >1 while the decreases were referred to negative values less than −1.

The $t_{max}$ change was defined as the difference between $(t_{max})_{sim}$ and $t_{max,std}$ as shown in equation (10).

$$t_{max} \text{ change} = t_{max,sim} - t_{max,std} \quad \text{(Eq. 10)}$$

where $t_{max,sim}$ was the value of $t_{max}$ in a specific simulation scenario.

**Fold Change Difference**. The differences between AUC fold change and $C_{max}$ fold change as shown in equation (11).

Fold change difference =

$$AUC \text{ fold change} - C_{max} \text{ fold change} \quad \text{(Eq. 11)}$$

### Data Analyses

#### Parameter Fold Change, Exposure Fold Change and Fold Change Difference Calculation

During the simulations, the parameter fold changes (including CL fold change, F fold change, $V_d$ fold change and $k_a$ fold change), the exposure fold changes (including AUC fold change, $C_{max}$ fold change and $t_{max}$ change) and the fold change difference were calculated for each scenario. Upon the iteration of the simulations,

**Table IV.** Model parameters for the second set of simulations

| Parameter | Value | Values with COMED | Justification |
|---|---|---|---|
| Dose (mg) | 5 | | One of the midazolam clinical dose |
| $k_a$ (1/h) | 1 | 0.2, 0.5, 1, 2, 5 | From low (1/5) to high (5×) around 1 |
| F | 0.2 | 0.05, 0.1, 0.2, 0.4, 1.0 | From low (1/5) to high (5×) around 0.2 |
| CL (L/h) | 38 | 7.6, 19, 38, 76, 190 | From low (1/5) to high (5×) around 38 |
| $V_d$ (L) | 260 | 52, 130, 260, 520, 1300 | From low (1/5) to high (5×) around 260 |

**CL** = clearance; **COMED** = concomitant medication; **F** = bioavailability; **$k_a$** = absorption rate constant; **$V_d$** = volume of distribution.

a data sheet was accumulated to record the parameters (CL, F, $V_d$ and $k_a$) used, resulted AUC, $C_{max}$ and $t_{max}$, and calculated parameter fold changes, exposure fold changes and fold change differences. The data sheet was used for generating plots.

### Plots Generation

Based on the results of the above calculations, the following plots were generated for the first set of simulations.

- The concentration-time profiles for all scenarios in each case were plotted.
- Exposure changes (including fold change difference, AUC fold change, Cmax fold change and $t_{max}$ change) were plotted against each parameter fold changes (including F fold change, CL fold change, $k_a$ fold change and $V_d$ fold change).

The following plots were generated for the second set of simulations.

- The fold change difference was plotted against each of the parameter fold changes to investigate the influencing parameters in the separation of $AUC_\infty$ fold changes and $C_{max}$ fold changes.
- The AUC fold change was plotted against each of the parameter fold changes.
- The $C_{max}$ fold change was plotted against each of the parameter fold changes.
- The $t_{max}$ change was plotted against each of the parameter fold changes.
- After the major influencing parameters were identified, the AUC fold change was examined against both CL fold change and F fold change in a 3-dimensional plot.

## Results

### The Simulated Profiles

For the first set of simulations, there were a total of 2400 concentration-time profiles accommodated in 96 pages. A representative page is shown in figure S1 in the Supplemental Digital Content 1, http://links.adisonline.com/DRZ/A1.

For the second set of simulations, the concentration-time profiles for each combination of different values of CL, F, $V_d$ and $k_a$ were gener-

ated. There were a total of 625 profiles accommodated in 25 pages. A representative page including the standard profile (using Standard Parameters, with a circle in the figure) is shown in figure S2 in the Supplemental Digital Content.

### The Effects of Parameter Fold Changes on Exposure Changes

For the first set of simulations, 96 plots for the exposure changes against parameter fold changes were generated. Figure 2 shows the plots of the exposure changes against CL fold changes for Cases 4–6 and Cases 10–12. Figure 3 shows the plots of the exposure changes against $V_d$ fold changes for Cases 13–15 and Cases 19–21. Figure 4 shows the plots of the exposure changes against $k_a$ fold changes for Cases 2, 5 and 11. Figure 5 shows the exposure changes against F fold changes for all cases.

The results from the second set were consistent with those from the first set of simulations. Figures S3–S6 in the Supplemental Digital Content show the effect of different parameter fold changes on AUC fold change, $C_{max}$ fold change, $t_{max}$ Change, and fold change difference, respectively.

### Area Under the Plasma Concentration versus Time Curve (AUC) Fold Change

For the first set of simulations, AUC fold change decreased with CL fold changes and increased with F fold changes, while it was not affected by $V_d$ fold changes and $k_a$ fold changes as shown in figures 2–5.

For the second set, figure S3 in the Supplemental Digital Content indicated that the AUC fold change was not affected by $k_a$ and $V_d$ evidenced by the fact that AUC fold change could be anywhere in the whole range regardless of $k_a$ fold change or $V_d$ fold change. As a result, AUC fold change would be determined by CL and F fold changes as shown in figure S7 in the Supplemental Digital Content. When CL fold change decreased to the lowest (−5-fold in the second set of simulations) and F fold change increased to the highest (5-fold in the second set of simulations), the AUC fold change was the most pronounced.
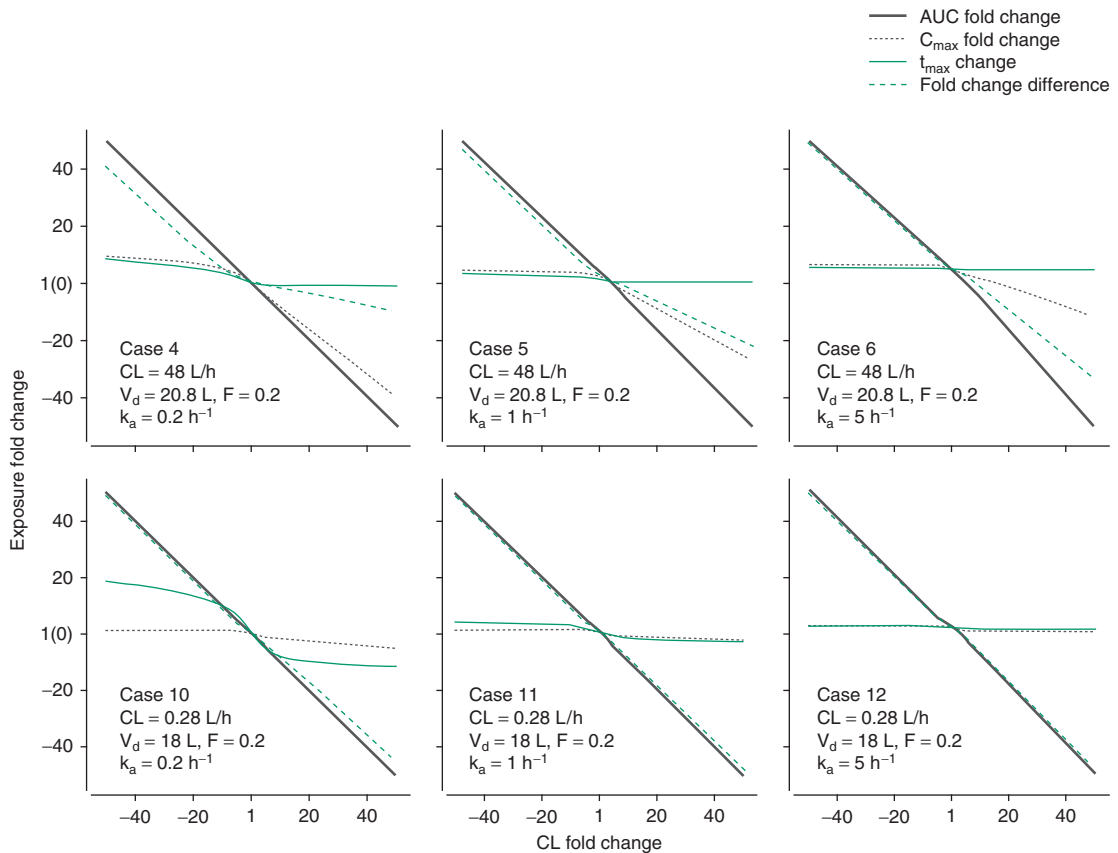
**Fig. 2.** The plots of area under the plasma concentration vs time curve (AUC) and maximum plasma concentration ($C_{max}$) fold changes, fold change difference and time to $C_{max}$ ($t_{max}$) change against clearance (CL) fold changes. The case number and corresponding standard parameters are labeled. Note that the y-axis labeled 1(0) indicates 1 for AUC fold change and $C_{max}$ fold change, while it is 0 for fold change difference and $t_{max}$. **F** = bioavailability; $k_a$ = absorption rate constant; $V_d$ = volume of distribution.

These effects were expected and straightforward according to equation (12).

$$AUC = \frac{F \times Dose}{CL} \qquad (Eq. 12)$$

### *Maximum Plasma Concentration ($C_{max}$) Fold Change*

$C_{max}$ fold change was more complex, which was the major factor accounting for the varied fold change difference.

The effect of F fold changes on $C_{max}$ fold change was the most obvious one. As shown in figure 5, $C_{max}$ fold change was proportional to F fold change. Since AUC fold change was also proportional to F fold change as shown in equa-

tion (12), if a DDI only caused F Change (no CL, $V_d$ or $k_a$ changes), the AUC fold change and $C_{max}$ fold change would be exactly the same and the fold change difference would be zero (figure 5). Although $C_{max}$ fold change was in the same direction as the F fold change, the exact proportionality was not shown as indicated in the upper right panel of figure S4 in the Supplemental Digital Content. The reason was that the second set of simulation used the same standard parameters and the resulted standard exposures for all possible combinations. Therefore, the relationships between the parameter fold changes and the exposure changes were in a range, not a single line. Due to the same reason,
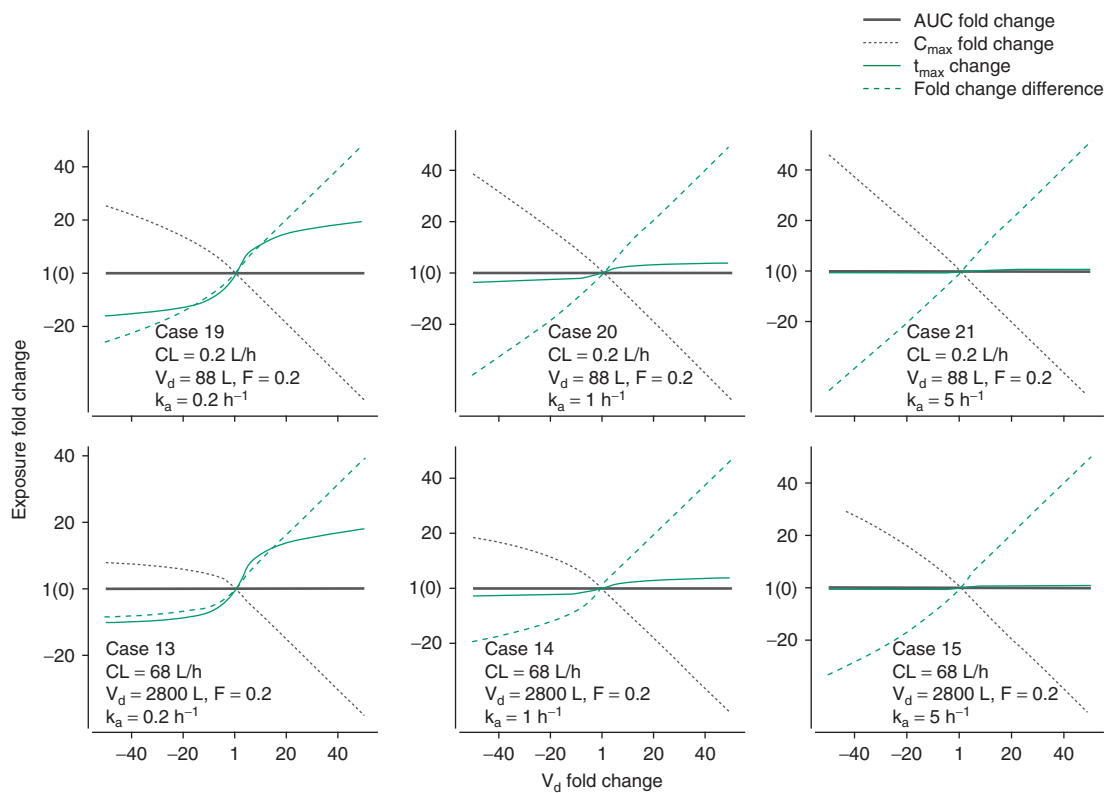
**Fig. 3.** The plots of area under the concentration curve (AUC) and maximum concentration ($C_{max}$) fold changes, fold change difference and time to $C_{max}$ ($t_{max}$) change against volume of distribution ($V_d$) fold changes. The case number and corresponding standard parameters are labeled. Note that the y-axis labeled 1(0) indicates 1 for AUC fold change and $C_{max}$ fold change while it is 0 for fold change difference and $t_{max}$ change. **F** = bioavailability; **$k_a$** = absorption constant.

unlike the one shown in figure 5, the relationship between the fold change difference and F fold change in the upper right panel in figure S6 in the Supplemental Digital Content was not a horizontal line.

The effect of CL fold change on $C_{max}$ fold change seemed generally small, especially for the drugs with long half-life and/or quick absorption. In figure 2, the difference in $C_{max}$ fold change among different panels can be appreciated. The lower three panels with longer half-life had minimal $C_{max}$ fold change, while for those in the upper row with shorter half-life, the $C_{max}$ fold change was significant. On the other hand, the panels on the left with smaller $k_a$ values showed larger $C_{max}$ fold change, while the panels on the right with larger $k_a$ values had smaller $C_{max}$ fold

change, with the panel at lower right corner having an almost straight horizontal line indicating little effect on the $C_{max}$ fold change. Another interesting fact was that the $C_{max}$ fold change resulting from an increase of CL fold change was quite different from that resulting from a decrease of CL fold change. Taking the panel at upper left corner as an example, increase of CL fold change caused decrease of $C_{max}$ fold change with a steep slope whereas decreases of CL fold change induced a shallow increase of $C_{max}$ fold change. This difference was not so obvious in the upper left panel of figure S4 in the Supplemental Digital Content due to two reasons: (i) the second set of simulation was taking Case 2 in the first set as basis and therefore the range was not wide enough; and (ii) the multiple

parameters were considered simultaneously, which may compensate for each other.

The effect of $k_a$ fold change on $C_{max}$ fold change was related to half-life as previously discussed and also as seen in figure 4. The standard parameter of $k_a$ was all the same ($1\,h^{-1}$) for the three panels in figure 4. The middle panel with shortest half-life produced the most prominent effect on $C_{max}$ fold change when $k_a$ fold change decreased, whereas the effect was much shallower for the right panel with longest half-life among the three cases. In addition, the different effects on $C_{max}$ fold change between the movement of $k_a$ fold change towards a positive direction (increase) and a negative direction (decrease) were observed. For the drugs with shorter half-life, the middle panel of figure 4, for example, the slope of the curve for the $C_{max}$ fold change against $k_a$ fold change in the negative direction was steep, while it was much shallower in the positive direction, and even leveled off in the other two panels. Since AUC fold change was not affected by $k_a$ fold change, the effect of $k_a$ fold change on the fold change difference was dependent on its effect on $C_{max}$ fold change. Roughly, the fold change difference curve was a mirror image of $C_{max}$ fold change, symmetric to the horizontal line at 1 (or 0).

A general trend between $k_a$ fold change and $C_{max}$ fold change consistent with this observation was seen for multiple parameter analysis as shown in the lower left panel in figure S4 in the Supplemental Digital Content.

The curve representing the effect of $V_d$ fold change on $C_{max}$ fold change was also related to half-life and $k_a$ fold change, especially the curve shape when the $V_d$ fold change moved to the negative direction as shown in figure 3. When the half-life was shorter and $k_a$ was smaller, this part of the curve leveled off as shown in the lower left panel. Along with the increase of half-life and $k_a$, the curve became steeper until it straightened up as shown in the upper right panel. Again, due to the stable AUC fold change, the curve for fold change difference was roughly a mirror image of the curve for $C_{max}$ fold change. When multiple parameters were considered simultaneously, the general trend between $V_d$ fold change and $C_{max}$ fold change was consistent with this observation as shown in the lower right panel of figures S4 and S6 in the Supplemental Digital Content.

### Time to Reach $C_{max}$ ($t_{max}$) Changes

Similar to $C_{max}$ fold change, $t_{max}$ change was affected by multiple parameters, although F fold
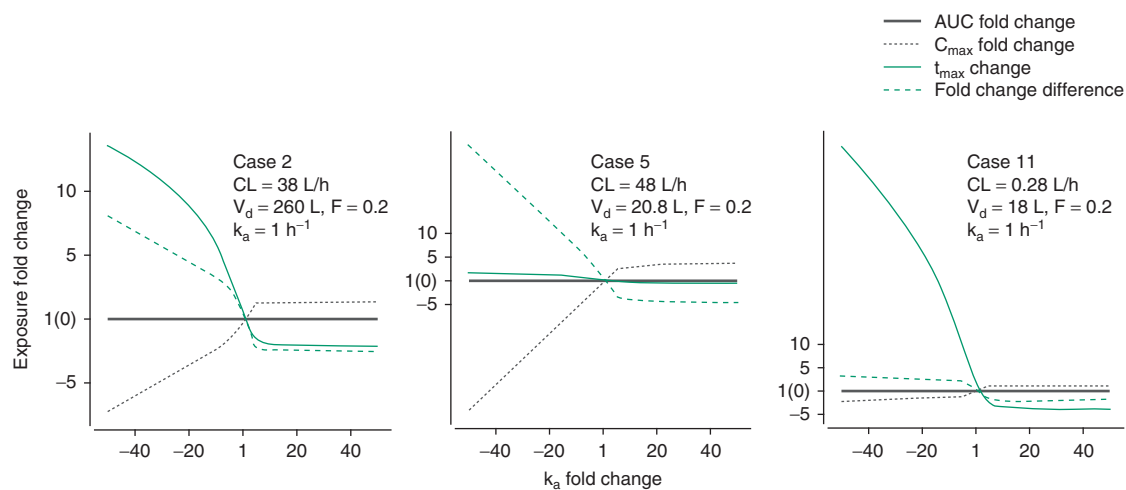


**Fig. 4.** The plots of area under the plasma concentration vs time curve (AUC) and maximum plasma concentration ($C_{max}$) fold changes, fold change difference, and time to $C_{max}$ ($t_{max}$) change against absorption rate constant ($k_a$) fold changes. The case number and corresponding standard parameters are labeled. Note that the y-axis labeled 1(0) indicates 1 for AUC fold change and $C_{max}$ fold change while it is 0 for fold change difference and $t_{max}$ change. **F** = bioavailability; **$V_d$** = volume of distribution.

change did not have any effect as shown in figure 5 and the upper right panel in figure S5 in the Supplemental Digital Content. Both the effects of CL fold change and $V_d$ fold change on $t_{max}$ change were dependent on $k_a$ values with smaller $k_a$ having more significant effects as shown in figures 2 and 3. Although the effects of half-life could be appreciated in these two figures, the effects were more prominent when the effects of $k_a$ fold change on $t_{max}$ change was considered. As shown in figure 4, for the drug with shorter half-life (the middle panel), $k_a$ fold change caused less $t_{max}$ change compared to the $t_{max}$ change for the drug with longer half-life (the right panel in figure S5 in the Supplemental Digital Content). For both cases, the negative $k_a$ fold change produced much larger $t_{max}$ change compared to the positive $k_a$ fold change as seen from both figure 4 and the lower left panel in figure S5 in the Supple-
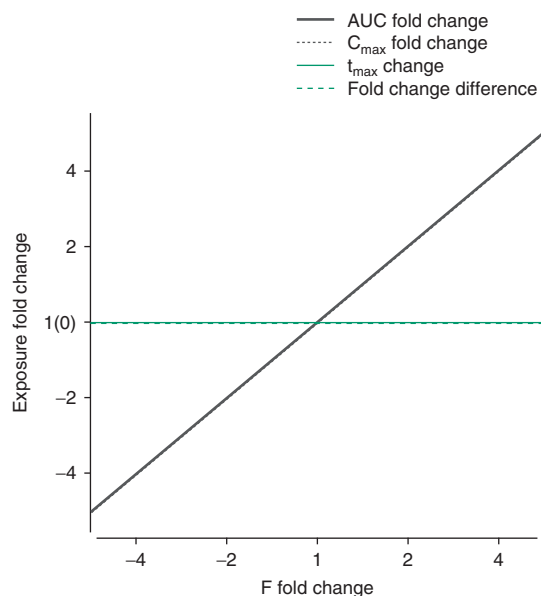


**Fig. 5.** The plots of area under the plasma concentration vs time curve (AUC) and maximum plasma concentration ($C_{max}$) fold changes, fold change difference, and time to $C_{max}$ ($t_{max}$) change against bioavailability (F) fold changes. Note that the y-axis labeled 1(0) indicates 1 for AUC fold change and $C_{max}$ fold change, while it is 0 for fold change difference and $t_{max}$ change. The diagonal lines for AUC fold changes and $C_{max}$ fold changes are overlapped, and the horizontal lines for fold change difference and $t_{max}$ changes are also overlapped.

mental Digital Content. It seemed that there was a threshold for the decrease of $t_{max}$ Change when the $k_a$ fold change going higher in the positive territory. The threshold value was also related to the half-life and the standard parameter of $k_a$ with smaller $k_a$ and longer half-life having more prominent threshold.

## Discussion

Due to the wide range of the fold changes of the primary parameters, the length of the sampling time was of concern to capture the major part of the profiles for the purpose of accurate calculations. As shown in figures S1 and S2 in the Supplemental Digital Content, most of the profiles were well within the length of the sampling time. Visual inspections for other pages for both the first and second set of simulations were conducted to ensure it was the case for all scenarios. However, it was the author's experience that the interval between adjacent sampling times was more important than the length of the sampling time. Because the accuracy of the calculations was of concern, the interval was set to 0.1 hour, which seemed to be adequate.

Instead of modeling for both the drug of interest and the COMED, the current approach examined the parameter changes of the drug of interest only. The purpose of the proposed approach is to get a general idea about the possible nature of the drug interaction by emphasizing the integration of all information available. The study provided visualizations for various exposure changes. The observations indicated that AUC was mainly influenced by CL and F, $C_{max}$ was affected by all four parameters, and $t_{max}$ was mainly affected by CL and $k_a$. F did little for $t_{max}$ and $k_a$ was unrelated to AUC. From each plot alone, limited information was obtained. To get better interpretation, an integration approach should be taken.

The study was conducted with concentration on the individual factor considered independently (the first set of the simulations), although multiple parameters were taken into account (in the second set of simulations). Indeed, the multiple parameter consideration was

more realistic and practical. For example, when the individual F fold change was considered independently, its effect on fold change difference showed a horizontal line (figure 5). However, when multiple parameters were taken into account simultaneously, the upper right panel in figure S6 in the Supplemental Digital Content provided a more realistic picture. Instead of a line, a broader range was given. More interestingly, the plot showed certain symmetry pattern. The symmetry of the effects of F fold change on the fold change difference in this case was caused by the symmetries of its effects on AUC fold changes (figure S3 in the Supplemental Digital Content) and $C_{max}$ fold changes (figure S4 in the Supplemental Digital Content). This symmetry had two possible consequences. First, at each level of F fold change, fold change difference had equal chances to go in either direction. For example, at level of 2 for F fold change, fold change difference ranged from about −10 to +10. The chances to go positive or negative were relatively equal dependent on the other parameters. Secondly, the increase or decrease of F fold change would have similar effects on fold change difference, with the centre point (F fold change = 1) having the smallest effect. For example, a 2-fold increase of F (F fold change = 2) would result in similar effects as it would for a 2-fold decrease of F (F fold change = −2). When F fold change was relatively small, the fold change difference would be smaller compared to the situation where F fold changes were larger (the upper right panel of figure S6 in the Supplemental Digital Content).

These consequences were important because when interpreting the data, one had to notice that a certain level of fold change difference observed could have been caused by either increased or decreased F fold changes.

With the importance of multiple parameter simultaneous consideration in mind, the following summary of the basic pattern of exposure changes according to the effects of parameter fold changes may be of help. Figure 6 was summarized from the 96 plots of the 24 cases studied. For the plot in each cell, the x-axis was the parameter fold changes and the y-axis was the exposure changes. The table can be read hor-
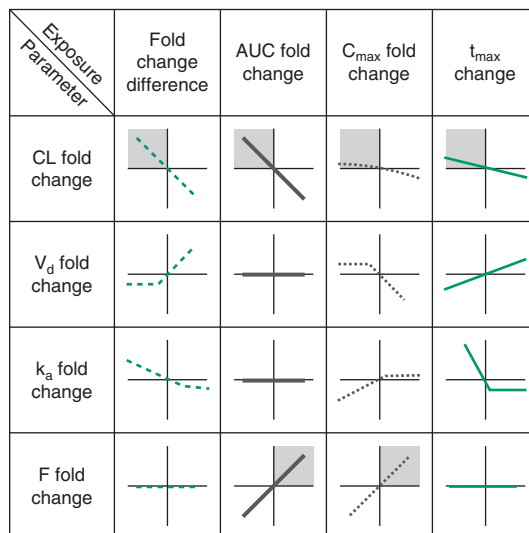


**Fig. 6.** Basic pattern summary and pattern reasoning. The columns and the ordinate in each cell show the exposure (fold change difference, area under the plasma concentration vs time curve [AUC] fold change, maximum plasma concentration [$C_{max}$] fold change and time to $C_{max}$ [$t_{max}$] change), while the rows and the abscissa in each cell show the parameter fold changes as labeled. The intersection of the ordinate and the abscissa represents the situations when parameter fold changes are 1 (no change). The right side from this point represents the parameter fold changes more than 1 (increase), while the left side stands for the parameter fold changes less than −1 (decrease). The line indicates the exposure changes (fold change difference, AUC fold change, $C_{max}$ fold change and $t_{max}$ change) when parameter fold changes increase (or decrease). Its slope signifies the extent of the changes. The shaded areas indicate the consistency of exposure changes induced by a specific parameter change, which provides the evidence for selecting the candidates for the example in the study by Hsu et al.[17]

izontally for each of the exposure changes affected by one of the parameter fold changes or vertically for the effects of each parameter fold changes on a specific exposure change. For example, reading horizontally for the effects of $V_d$ fold change would result in the following.

- Decreased $V_d$ fold change would cause a small decrease of fold change difference, no effect on AUC fold change, a small increase of $C_{max}$ fold change and a modest decrease of $t_{max}$ change.
- Increased $V_d$ fold would cause an increase of fold change difference, no effect on AUC fold change, a decrease of $C_{max}$ fold change and a modest increase of $t_{max}$ change.

To use this chart to interpret DDI, follow the steps below. For the purpose of illustration, the

DDI of saquinavir with coadministration of ritonavir[17] is taken as an example.

1. Perform a drug interaction study and get the values of AUC, $C_{max}$ and $t_{max}$ in the presence and the absence of COMED.

2. Calculate the AUC fold change, $C_{max}$ fold change and $t_{max}$ change. Get the fold change difference. In the example, AUC fold change is 128.9, $C_{max}$ fold change is 32.5, $t_{max}$ change is 0.8 h and the fold change difference is 96.4.

3. Find the candidates of parameter fold changes, which account for the exposure changes obtained from step 2. In the example, all the exposure changes are positive. For this reason, CL fold change could be a candidate because decreased CL fold change would make all exposure changes positive. However, $V_d$ fold change may not qualify the candidacy due to the fact that although decreased $V_d$ fold change could cause an increase of $C_{max}$ fold change, it would result in decreases of $t_{max}$ change and fold change difference based on figure 6. On the other hand, although an increase of $V_d$ fold change could make $t_{max}$ change and fold change difference positive, it would induce a decrease of $C_{max}$ fold change. In addition, the increase of AUC fold change is so significant in the example, while figure 6 shows no change of AUC when $V_d$ fold change is altered. For the similar reasons, $k_a$ fold change may be eliminated from the candidate list. It is noted that there is a significant increase of $C_{max}$ fold change (32.5). If reading the chart vertically for the column of $C_{max}$ fold change, significant increase of $C_{max}$ fold change only occurs when there is an increase of F fold change. Therefore, although the increase of F fold change alone may not produce increases of $t_{max}$ change and fold change difference, its contribution could not be ignored due to the considerable increase of $C_{max}$ fold change. Therefore, two potential candidates are selected. The reasoning process can be found by the shaded areas in figure 6.

4. Consider all available information to confirm or reject the candidates. For the example, saquinavir is primarily eliminated by means of metabolism; only 3% of a $^{14}$C-labelled dose is recovered in urine after intravenous administration.[23] In addition, the reported systemic plasma CL of saquinavir is higher than hepatic plasma flow. The absolute oral bioavailability of saquinavir is about 3%. Cytochrome P450 (CYP) 3A, the major isoform in the metabolism of ritonavir and saquinavir is present in intestinal tissue,[24,25] in addition to the liver. Thus, it is likely that saquinavir undergoes first-pass metabolism by both intestinal and hepatic enzymes. Because of this, coupled with the fact that ritonavir has a low *in vitro* concentration that produced 50% inhibition ($IC_{50}$), it would be expected that ritonavir would have a marked inhibitory effect on the first-pass metabolism of saquinavir. In contrast, because the plasma CL of saquinavir approaches or exceeds hepatic plasma flow rate, even though ritonavir has a low *in vitro* $IC_{50}$, it is likely that the post-absorptive inhibition effect will not be large. The information listed here tends to confirm the candidates selected by figure 6. However, the apparent controversy between a large AUC fold change (128.9) and the relatively small effects of CL fold change implied by the statements that the post-absorptive inhibition effect will not be large needs more explanation. Since the effects of CL fold change on $C_{max}$ fold change are generally small (figure 2), one may assume that the effect observed for the $C_{max}$ fold change of saquinavir is primarily caused by F fold change (i.e. the suppression of the first-pass metabolism). Ritonavir would then yield a significant inhibition of the first-pass metabolism, resulting in a $C_{max}$ fold change of 32.5 and also an AUC fold change of 32.5. If the net effect on AUC is the product of first-pass and post-absorptive inhibition, then the latter corresponding inhibition can be estimated to be 4 expressed as the AUC fold change, which is relatively small and very close to the reported estimate.[17]

It is important to understand the nature of DDI in order to prevent its adverse consequences if any. When a DDI is metabolism based, it is critical to identify whether the DDI occurs at pre-systemic level or systemic level. One of the difficulties for such an interpretation is that the absolute bioavailability (F) of a drug is usually not readily available and furthermore, it is difficult to estimate the F changes during a DDI

study. As a result, the proposed approach to perform a rough estimate seems attractive. The following potential applications of such a pattern recognition approach may be anticipated.

1. A general understanding and a rough estimate about the nature of the DDI observed may be obtained from a simple comparison.

2. Based on the understanding of the mechanism, the output can be predicted regarding which exposure index is more prominent when it is of concern. As mentioned earlier, for some drugs, AUC is the major concern of exposure and for others it is $C_{max}$. Under certain circumstances, $t_{max}$ is also of concern.

3. This approach would be helpful to understand any situation where AUC and $C_{max}$ have differences, such as providing an explanation for a failed bioequivalence study. In one scenario, the AUC meets the criteria but $C_{max}$ does not, while under another scenario, $C_{max}$ meets the criteria but AUC does not. The pattern recognition approach would suggest helpful hints to single out the possible mechanism in order to decide whether the differences between the test and reference are caused by the formulation differences or some other influential factors. By the same token, this pattern recognition approach would also be useful for interpretations of other similar studies, such as food effect study (with and without food), renal impairment and hepatic impairment studies (subject groups with different renal or hepatic functions), where the AUC and $C_{max}$ changes differ and $t_{max}$ varies.

4. The approach would be beneficial for interpreting the exposure difference resulting from different genetic makeup. For example, poor metabolizers of CYP2D6 have a 10-fold higher AUC and a 5-fold higher peak concentration to a given dose of atomoxetine compared with extensive metabolizers.[14]

5. Manufacture parameters may affect the *in vivo* performance. The pattern recognition approach will help the understanding of the effects of the manufacture parameters.

It should be emphasized that this approach be integrated with other methodologies due to its limited abilities. The limitations for the current study are listed below.

1. A linear, one-compartment model with first-order elimination was assumed. The real world might be more complex. When metabolism-based DDI is considered, saturation is frequently observed. The drugs listed in table I might not all follow the assumptions. With emphasizing the general trend for common parameters related to drug absorption, bioavailability and elimination, caution should be exercised for assumption violation.

2. The first-order absorption was used (constant $k_a$). It implied the unrealistic assumption that the maximum absorption rate was achieved instantaneously. Due to its popularity and the fact that in some cases it was sufficient to describe the process of drug input, the current study used it for easier interpretation.

3. Lag time, the delay between drug administration and the beginning of absorption, was not considered in this study. The lag time can be anywhere from a few minutes to many hours. It may be particularly important when a rapid onset of effect is desired.

4. Single dose was used in all the simulations. Multiple doses might be needed to show a significant interaction. However, considering that the purpose of this study was to compare the exposure between the subjects with COMED and those without, the single dose results could be extrapolated to the case of multiple doses with a linear assumption.

5. The results obtained from this approach could be inconclusive. However, a general trend is helpful, in principle. Furthermore, integration with other methodologies for interpretation is always advised.

## Conclusion

With the assumptions that the primary parameters of a drug of interest are altered during a DDI, an approach, named DDI pattern recognition for didactical purposes, is proposed for interpreting the DDI results based on the exposure fold changes. DDI pattern recognition may provide an insight of the mechanistic nature of DDI and a general idea about the processes, which dominate a DDI.

This approach analyses DDI from a new angle. Due to the complexity of DDI, one angle is not enough. By emphasizing the integration of all available information and mechanistic interpretation from multiple angles, the new approach may play a significant role in interpreting DDI studies.

## Acknowledgments

## References

1. Gibaldi N, Perrier D. Pharmacokinetics. 2nd ed. New York (NY): Plenum Publishing Corp, 1982
2. Rakhit A, Pantze MP, Fettner S, et al. The effects of CYP3A4 inhibition on erlotinib pharmacokinetics: computer-based simulation (SimCYP) predicts in vivo metabolic inhibition. Eur J Clin Pharmacol 2008; 64: 31-41
3. Laine K, Anttila M, Helminen A, et al. Dose linearity study of selegiline pharmacokinetics after oral administration: evidence for strong drug interaction with female sex steroids. Br J Clin Pharmacol 1999; 47: 249-54
4. Guns ES, Denyssevych T, Dixon R, et al. Drug interaction studies between paclitaxel (Taxol) and OC144-093: a new modulator of MDR in cancer chemotherapy. Eur J Drug Metab Pharmacokinet 2002; 27: 119-26
5. Thomson Micromedex. Physicians' desk reference (electronic version). Gleevec® (imatinib mesylate) tablets (Novartis). Greenwood Village (CO): Thomson Micromedex, 2009
6. Schneck DW, Birmingham BK, Zalikowski JA, et al. The effect of gemfibrozil on the pharmacokinetics of rosuvastatin. Clin Pharmacol Ther 2004; 75: 455-63
7. Kiser JJ, Gerber JG, Predhomme JA, et al. Drug/Drug interaction between lopinavir/ritonavir and rosuvastatin in healthy volunteers. J Acquir Immune Defic Syndr 2008; 47: 570-8
8. Simonson SG, Raza A, Martin PD, et al. Rosuvastatin pharmacokinetics in heart transplant recipients administered an antirejection regimen including cyclosporine. Clin Pharmacol Ther 2004; 76: 167-77
9. Kovarik JM, Kalbag J, Figueiredo J, et al. Differential influence of two cyclosporine formulations on everolimus pharmacokinetics: a clinically relevant pharmacokinetic interaction. J Clin Pharmacol 2002; 42: 95-9
10. Yasui-Furukori N, Saito M, Inoue Y, et al. Terbinafine increases the plasma concentration of paroxetine after a single oral administration of paroxetine in healthy subjects. Eur J Clin Pharmacol 2007; 63: 51-6
11. Thomson Micromedex. Physicians' desk reference (electronic version). LAMISIL® (terbinafine hydrochloride) oral granules (Novartis). Greenwood Village (CO): Thomson Micromedex, 2009
12. Thomson Micromedex. Physicians' desk reference (electronic version). CYMBALTA® (duloxetine hydrochloride) delayed release capsules (Lilly). Greenwood Village (CO): Thomson Micromedex, 2009
13. Moody DE, Walsh SL, Rollins DE, et al. Ketoconazole, a cytochrome P450 3A4 inhibitor, markedly increases concentrations of levo-acetyl-alpha-methadol in opioid-naive individuals. Clin Pharmacol Ther 2004; 76: 154-66
14. Thomson Micromedex. Physicians' desk reference (electronic version). STRATTERA® (atomoxetine hydrochloride) capsules for oral use (Lilly). Greenwood Village (CO): Thomson Micromedex, 2009
15. Tornio A, Niemi M, Neuvonen M, et al. The effect of gemfibrozil on repaglinide pharmacokinetics persists for at least 12 h after the dose: evidence for mechanism-based inhibition of CYP2C8 in vivo. Clin Pharmacol Ther 2008; 84: 403-11
16. Moton A, Ma L, Krishna G, et al. Effects of oral posaconazole on the pharmacokinetics of sirolimus. Curr Med Res Opin 2009; 25: 701-7
17. Hsu A, Granneman GR, Cao G, et al. Pharmacokinetic interactions between two human immunodeficiency virus protease inhibitors, ritonavir and saquinavir. Clin Pharmacol Ther 1998; 63: 453-64
18. Thomson Micromedex. Physicians' desk reference (electronic version). Advair Diskus® (fluticasone propionate, salmeterol xinafoate) 100/50 (GlaxoSmithKline). Greenwood Village (CO): Thomson Micromedex, 2009
19. Wendrow A. Drug Combinations quick reference guide. 6-1-2000 [online]. Available from URL: http://www.thefreelibrary.com/_/print/PrintArticle.aspx?id=65014034 [Accessed 2010 Apr 30]
20. Ebert U, Oertel R, Kirch W. Influence of grapefruit juice on scopolamine pharmacokinetics and pharmacodynamics in healthy male and female subjects. Int J Clin Pharmacol Ther 2000; 38: 523-31
21. Food and Drug Administration. Guidance for industry drug interaction studies: study design, data analysis, and implications for dosing and labeling. Silver Spring (MD): FDA, 2006
22. Tozer TN. Concepts basic to pharmacokinetics. Pharmacol Ther 1981; 12: 109-31
23. Schapiro JM, Winters MA, Stewart F, et al. The effect of high-dose saquinavir on viral load and CD4+ T-cell counts in HIV-infected patients. Ann Intern Med 1996; 124: 1039-50
24. Watkins PB, Wrighton SA, Schuetz EG, et al. Identification of glucocorticoid-inducible cytochromes P-450 in the intestinal mucosa of rats and man. J Clin Invest 1987; 80: 1029-36
25. Kolars JC, Lown KS, Schmiedlin-Ren P, et al. CYP3A gene expression in human gut epithelium. Pharmacogenetics 1994; 4: 247-59

Correspondence: Dr *John Z. Duan*, FDA/CDER/OPS/ONDQA, WO Bldg 21 Room 1616, 10903 New Hampshire Ave., Silver Spring, MD 20993, USA.
E-mail: john.duan@fda.hhs.gov